

Gene expression profiling analysis of lung adenocarcinoma

H. Xu^{1,2}, J. Ma¹, J. Wu¹, L. Chen¹, F. Sun¹, C. Qu¹, D. Zheng¹ and S. Xu¹

¹Department of Thoracic Surgery, Harbin Medical University Cancer Hospital, Harbin, Heilongjiang, China

²Laboratory of Medical Genetics, Harbin Medical University, Harbin, Heilongjiang, China

Abstract

The present study screened potential genes related to lung adenocarcinoma, with the aim of further understanding disease pathogenesis. The GSE2514 dataset including 20 lung adenocarcinoma and 19 adjacent normal tissue samples from 10 patients with lung adenocarcinoma aged 45-73 years was downloaded from Gene Expression Omnibus. Differentially expressed genes (DEGs) between the two groups were screened using the *t*-test. Potential gene functions were predicted using functional and pathway enrichment analysis, and protein-protein interaction (PPI) networks obtained from the STRING database were constructed with Cytoscape. Module analysis of PPI networks was performed through MCODE in Cytoscape. In total, 535 upregulated and 465 downregulated DEGs were identified. These included *ATP5D*, *UQCRC2*, *UQCRC1* and genes encoding nicotinamide adenine dinucleotide (NADH), which are mainly associated with mitochondrial ATP synthesis coupled electron transport, and which were enriched in the oxidative phosphorylation pathway. Other DEGs were associated with DNA replication (*PRIM1*, *MCM3*, and *RNASEH2A*), cell surface receptor-linked signal transduction and the enzyme-linked receptor protein signaling pathway (*MAPK1*, *STAT3*, *RAF1*, and *JAK1*), and regulation of the cytoskeleton and phosphatidylinositol signaling system (*PIP5K1B*, *PIP5K1C*, and *PIP4K2B*). Our findings suggest that DEGs encoding subunits of NADH, *PRIM1*, *MCM3*, *MAPK1*, *STAT3*, *RAF1*, and *JAK1* might be associated with the development of lung adenocarcinoma.

Key words: Lung adenocarcinoma; Pathogenesis; Differentially expressed genes; Protein-protein interaction; Network module

Introduction

Lung cancer is the leading cause of cancer deaths among men and women worldwide. The incidence of lung cancer has shown a rising trend in China, with an average annual growth of 1.63% (1). Pathologically, lung cancer can be divided into small cell and the more common non-small cell histological types. The survival prognosis of non-small cell lung cancer (NSCLC) patients is extremely poor, with an average annual 5-year survival rate of less than 15% (2).

The development of lung adenocarcinoma is a multi-factor and multistage process, with genetic instability considered to be the key cause. In recent years, important progress has been made in understanding the molecular mechanism of lung adenocarcinoma. Kris et al. (3) reported that 60% (252/422) of lung adenocarcinoma tissues harbor a driver mutation, including those in genes encoding Kirsten rat sarcoma viral oncogene (*KRAS*; 25%), epidermal growth factor receptor (*EGFR*; 23%), anaplastic lymphoma kinase (*ALK*; 6%) and proto-oncogene B-Raf (*BRAF*; 3%). Among these, the *EGFR* pathway is the main signaling pathway of lung cancer, and the mutation rate of its genes reaches 70%-80% (4). *EGFR* mutations are usually heterozygotic because the mutant allele is also coupled with gene

amplification. The kinase activity increase of *EGFR* can lead to the hyperactivation of downstream signal pathways that enhance cell survival. *KRAS* mutations account for 30%–35% of lung adenocarcinoma genetic variation (5). Around 97% of *KRAS* mutations in NSCLC occur in codons 12 or 13 (6), and Mills et al. (7) have shown that the sensitive detection of *KRAS* codon 12 mutations in bronchoalveolar lavage can help diagnose lung cancer. *ALK* fusions are observed in ~4% of NSCLC patients (8), resulting from an inversion of *EML4* and *ALK* gene on the short arm of chromosome 2 which constitutively activates the kinase and protein oligomerization (9).

As well as the above genes and pathways, other molecular changes can bring about lung adenocarcinoma, such as mutations in *ROS* (10,11), *ERCC1* (12), *RB* (13), *AKT* (14), *PTEN* (15), and *MAP2K1* (16). Stearman et al. (17) compared orthologous gene expression between human pulmonary adenocarcinoma and a urethane-induced murine model, and identified 409 gene classifiers that showed significant ($P < 0.0001$) and positive correlation in expression between the two species. Moreover, the detection of prosta-cyclin synthase was found to have a significant prognostic

Correspondence: S. Xu: <shidongxuxu@163.com>

Received April 15, 2015 | Accepted August 5, 2015

value in patient survival. However, no further investigations have been carried out into changes in metabolic pathways or genes involved in human lung adenocarcinoma.

In this study, therefore, we aimed to obtain an improved insight into lung adenocarcinoma by searching microarray data for differentially expressed genes (DEGs) between lung adenocarcinoma and adjacent normal tissue samples. We also constructed a protein-protein interaction (PPI) network, and performed functional and pathway enrichment analyses of network modules.

Material and Methods

Affymetrix microarray data

The expression profile data of GSE2514 were obtained from a public functional genomics data repository Gene Expression Omnibus (GEO) database (<http://www.ncbi.nlm.nih.gov/geo/>) (17), which was based on the platform of the Affymetrix Human Genome U95 Version 2 Array. A total of 39 human tissue samples were available for further analysis, of which 20 were lung adenocarcinoma samples and 19 were adjacent normal tissue samples from five males and five females with lung adenocarcinoma, aged 45–73 years. All patients participating in this study were enrolled in a protocol approved by the local Colorado Multiple Institutional Review Board for the use of remnant tissues with anonymization and analysis of specimens and clinical data. Tumors were histologically classified according to World Health Organization guidelines and staged according to the tumor-node-metastasis classification. With the exception of two stage III tumors, most tumors were low stage and low to intermediate grade.

Affymetrix CEL files and probe annotation files were downloaded, and gene expression data of all samples were preprocessed using the GeneChip Robust Multi Array algorithm in the Affy software package (18).

DEG screening

The *t*-test was used to identify genes that were significantly differentially expressed between lung tumor samples and adjacent normal tissue samples. The raw *P*-value was adjusted by the Benjamin and Hochberg method (19), and only genes following the cut-off criteria of $[\log_2FC \text{ (fold change)}] > 0.5$ and adjusted $P < 0.05$ were selected as DEGs.

Gene ontology (GO) and pathway enrichment analyses

The Database for Annotation, Visualization and Integrated Discovery (DAVID) gene functional classification database now provides a set of comprehensive functional annotation tools for investigators to comprehend the biological meanings behind many genes. Kyoto Encyclopedia of Genes and Genomes (KEGG) pathway enrichment analysis (20) was conducted to identify significant pathways for DEGs. A $P < 0.05$ was used as the cut-off criterion for GO

and KEGG pathway enrichment analyses using default parameters by DAVID.

PPI network construction

The Search Tool for the Retrieval of Interacting Genes (STRING) database provides both experimental and predicted interaction information. This database was used to analyze PPIs for DEGs by calculating their Required Confidence score; a score > 0.4 was chosen as the cut-off criterion. PPI networks of upregulated and downregulated DEGs were then respectively visualized by Cytoscape (<http://cytoscape.org/>), which is an open source software for visualizing complex networks and integrating them with any type of attribute data. Hub proteins (essential high-degree proteins in PPI networks) (21,22) were found by counting the connectivity degree of each network node based on the scale-free property of interaction networks. The connectivity degree of each node represents the number of interactions the node has with other nodes.

Screening and analysis of network modules

Network modules were obtained based on the MCODE analysis of original PPI networks. Default parameters (Degree Cutoff: 2, Node Score Cutoff: 0.2, K-Core: 2, Max. Depth: 100) were used as the cut-off criteria for network module screening.

To obtain a better understanding at the molecular level of gene function and to identify pathways closely associated with DEGs, the functional annotation and pathway enrichment analysis of network modules with higher MCODE scores were performed using online DAVID software with a threshold of $P < 0.05$.

Results

DEGs between lung tumor and healthy lung tissue cells

After data preprocessing, 11,551 probes were obtained. Based on the cut-off criteria, 1000 DEGs including 535 that were upregulated and 465 downregulated were screened.

GO and KEGG pathway enrichment analyses of upregulated and downregulated DEGs

GO terms of upregulated DEGs were significantly related to RNA processing ($P=3.89E-09$), RNA splicing ($P=3.27E-07$), oxidative phosphorylation ($P=3.51E-07$), and the electron transport chain ($P=6.76E-07$; Supplementary Table S1). GO terms of downregulated DEGs were mainly related to the regulation of cell motion ($P=7.21E-05$), morphogenesis of a branching structure ($P=8.02E-05$), and lung development ($P=7.37E-04$; Supplementary Table S2).

Upregulated DEGs were enriched in 11 pathways, and most significantly in oxidative phosphorylation ($P=4.67E-07$), Parkinson's disease ($P=5.63E-07$), and Huntington's disease ($P=1.11E-05$; Figure 1A), while downregulated DEGs

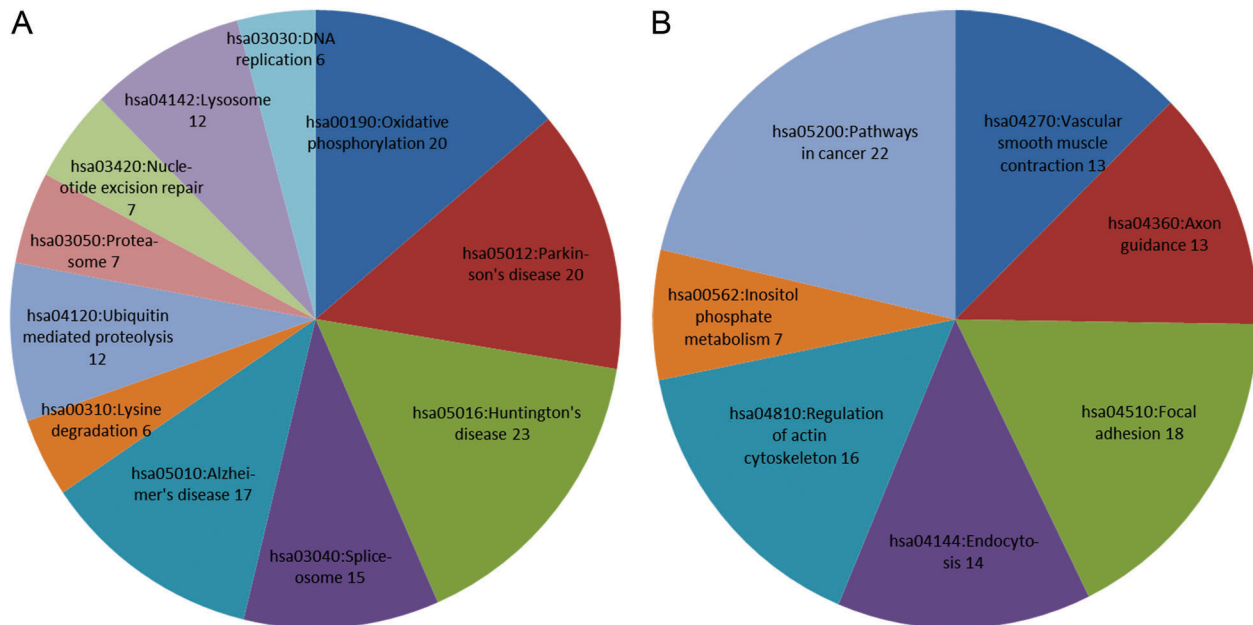


Figure 1. KEGG pathway enrichment analysis for upregulated differentially expressed genes (A) and downregulated differentially expressed genes (B).

were enriched in seven pathways, most significantly in vascular smooth muscle contraction ($P=1.29E-03$), axon guidance ($P=3.80E-03$), and focal adhesion ($P=6.74E-03$; Figure 1B).

Construction and analysis of PPI networks

PPI networks for upregulated and downregulated DEGs consisted of 1,591 and 661 pairs of PPIs, respectively (Figure 2A and B).

The connectivity degree of certain genes exceeded 20, including *DHX15*, *NDUFS3*, *PSMC6*, *UBE2C*, *EIF4G1*, *DHX9*, *PSMC3*, and *HNRNPA2B1* in the upregulated PPI network, and *MAPK1*, *IL6*, *FN1*, *MAPK14*, *STAT3*, and *VWF* in the downregulated PPI network (Table 1).

Analysis of network modules

A total of 24 modules including 14 upregulated and 10 downregulated network modules were obtained using default criteria. Among these, five upregulated modules (up-1, up-2, up-3, up-4, and up-5) with nodes >5 and a MCODE score >6 (Figure 3), and six downregulated modules (d-1, d-2, d-3, d-4, d-5, and d-6) with nodes >3 and a MCODE score >3 (Figure 4) were selected for enrichment analysis.

Functional enrichment analysis for two upregulated modules (up-1 and up-2) with a higher enrichment score showed that the genes in module up-1 (e.g., *DHX9*, *HNRNPA2B1*, *HNRNPR*, *GTF2F2*, and *SNRNP40*) were mainly enriched in RNA splicing ($P=1.53E-17$) and mRNA

processing ($P=3.94E-14$) pathways. Genes in module up-2 (*ATP5D*, *UQCRC2*, *NDUFS7*, *NDUFA2*, *UQCR11*, *NDUFB8*, *NDUFV1*, *NDUFV2*, *NDUFA7*, *NDUFS3*, *NDUFA1*, and *NDUFB1*) were mainly related to mitochondrial ATP synthesis coupled electron transport ($P=1.12E-14$), the electron transport chain ($P=7.35E-14$), and mitochondrial electron transport ($P=9.94E-14$; Table 2). There were no significant GO terms for genes in modules up-3 or up-4; moreover, the enrichment score of module up-5 was much lower than that of modules up-1 and up-2, so module up-5 GO terms are not listed in Table 2.

Because of their higher enrichment scores and gene numbers, modules up-1 and up-2 were selected for further pathway enrichment analysis. DEGs in module up-1, such as *POLR2G*, *POLR2F*, *DDX23*, *PRIM1*, *MCM3*, *TK1*, *SNRNP40*, *SNRNP70*, and *RNASEH2A*, were significantly enriched in three pathways of pyrimidine metabolism ($P=1.15E-03$), DNA replication ($P=5.24E-03$), and spliceosome ($P=4.41E-02$). DEGs in module up-2, such as *ATP5D*, *UQCRC2*, *NDUFA2*, *NDUFB8*, *NDUFA7*, *COX4I1*, *NDUFA1*, *NDUFB1*, *NDUFS7*, *UQCR11*, *NDUFV1*, *NDUFV2*, and *NDUFS3*, were enriched in the pathways of oxidative phosphorylation ($P=3.31E-13$), Parkinson's disease ($P=3.81E-13$), Alzheimer's disease ($P=3.25E-11$), and Huntington's disease ($P=7.35E-11$; Table 3).

The enriched functions for genes in two downregulated modules (d-1 and d-5) with higher enrichment scores showed that genes in module d-1 (e.g., *MAPK1*, *MAPK14*, *MITF*, *RAF1*, *JAK1*, *HBEGF*, *ROS1*, and *STAT3*) were

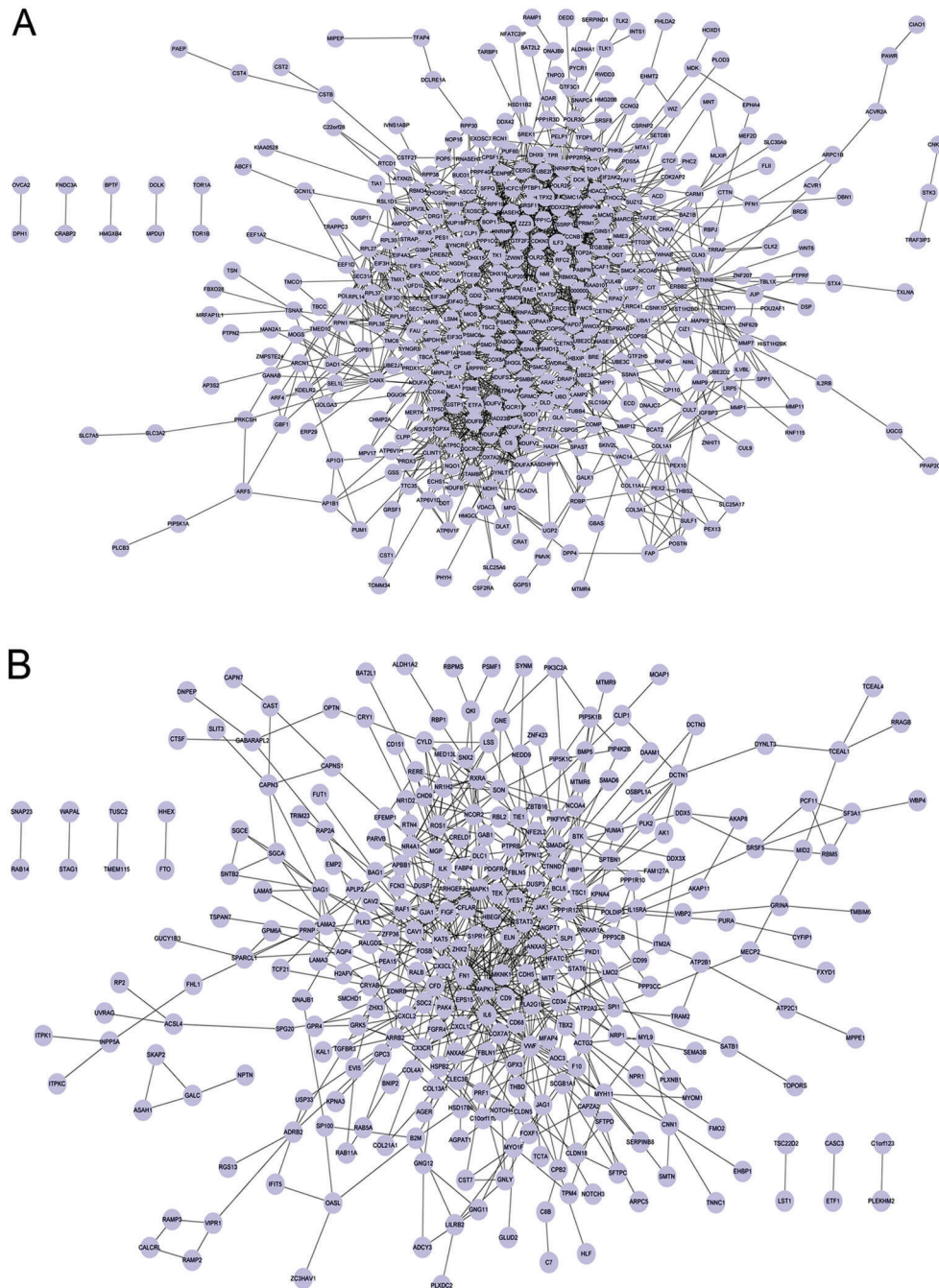


Figure 2. Protein-protein interaction network for upregulated differentially expressed genes (A) and downregulated differentially expressed genes (B).

related to cell surface receptor linked signal transduction ($P=1.71E-03$), and enzyme-linked receptor protein signaling pathway ($P=2.02E-03$); while genes in module d-5 (e.g., *PIP5K1B*, *PIP5K1C*, *PIP4K2B*, *CXCL12*, and *FN1*) were mainly enriched in phosphatidylinositol metabolic processes ($P=4.24E-04$), glycerolipid metabolic processes

($P=1.88E-03$), and cell morphogenesis ($P=2.06E-02$; Table 4). There were no significant GO terms for genes in modules d-2, d-3, d-4, or d-6.

Similarly, because of their higher enrichment scores and gene numbers, modules d-1 and d-5 were selected for further pathway enrichment analysis. Five pathways

Table 1. Differentially expressed genes with the top 10% connectivity degree in upregulated and downregulated protein-protein interaction networks.

Network	ID	Degree	ID	Degree	ID	Degree	ID	Degree	
Upregulated	<i>DHX15</i>	28	<i>SRSF11</i>	20	<i>NDUFB8</i>	18	<i>RPL30</i>	16	
	<i>NDUFS3</i>	26	<i>GTF2F2</i>	20	<i>PAICS</i>	18	<i>PTBP1</i>	16	
	<i>PSMC6</i>	25	<i>CPSF1</i>	20	<i>UQCR11</i>	18	<i>MCM3</i>	16	
	<i>UBE2C</i>	25	<i>NDUFV1</i>	19	<i>PRIM1</i>	18	<i>ZWINT</i>	16	
	<i>EIF4G1</i>	24	<i>SNRNP70</i>	19	<i>HNRNPR</i>	18	<i>ATP5D</i>	16	
	<i>DHX9</i>	23	<i>PSMD10</i>	19	<i>EIF3G</i>	17	<i>SNRNP40</i>	16	
	<i>PSMC3</i>	23	<i>SMC1A</i>	19	<i>NDUFV2</i>	17	<i>PABPN1</i>	16	
	<i>HNRNPA2B1</i>	22	<i>CCNB1</i>	19	<i>COX4I1</i>	17	<i>TOP1</i>	16	
	<i>POLR2G</i>	21	<i>UQCRC2</i>	18	<i>EIF4A3</i>	17	<i>RNASEH2A</i>	16	
	<i>TOP2A</i>	21	<i>POLR2F</i>	18	<i>NDUFA1</i>	17			
	<i>PSMB6</i>	21	<i>DDX23</i>	18	<i>FAU</i>	16			
	Downregulated	<i>MAPK1</i>	41	<i>CD34</i>	19	<i>RAF1</i>	13	<i>ELN</i>	12
		<i>IL6</i>	33	<i>HBEGF</i>	16	<i>BCL6</i>	13	<i>ANGPT1</i>	11
		<i>FN1</i>	32	<i>CAV1</i>	16	<i>ARRB2</i>	13	<i>MGP</i>	11
<i>MAPK14</i>		25	<i>ZHX2</i>	15	<i>RXRA</i>	12	<i>SMAD4</i>	11	
<i>STAT3</i>		22	<i>CXCL12</i>	14	<i>JAK1</i>	12	<i>NR1H2</i>	11	
<i>VWF</i>		20	<i>NCOR2</i>	14	<i>CDH5</i>	12	<i>SDC2</i>	11	

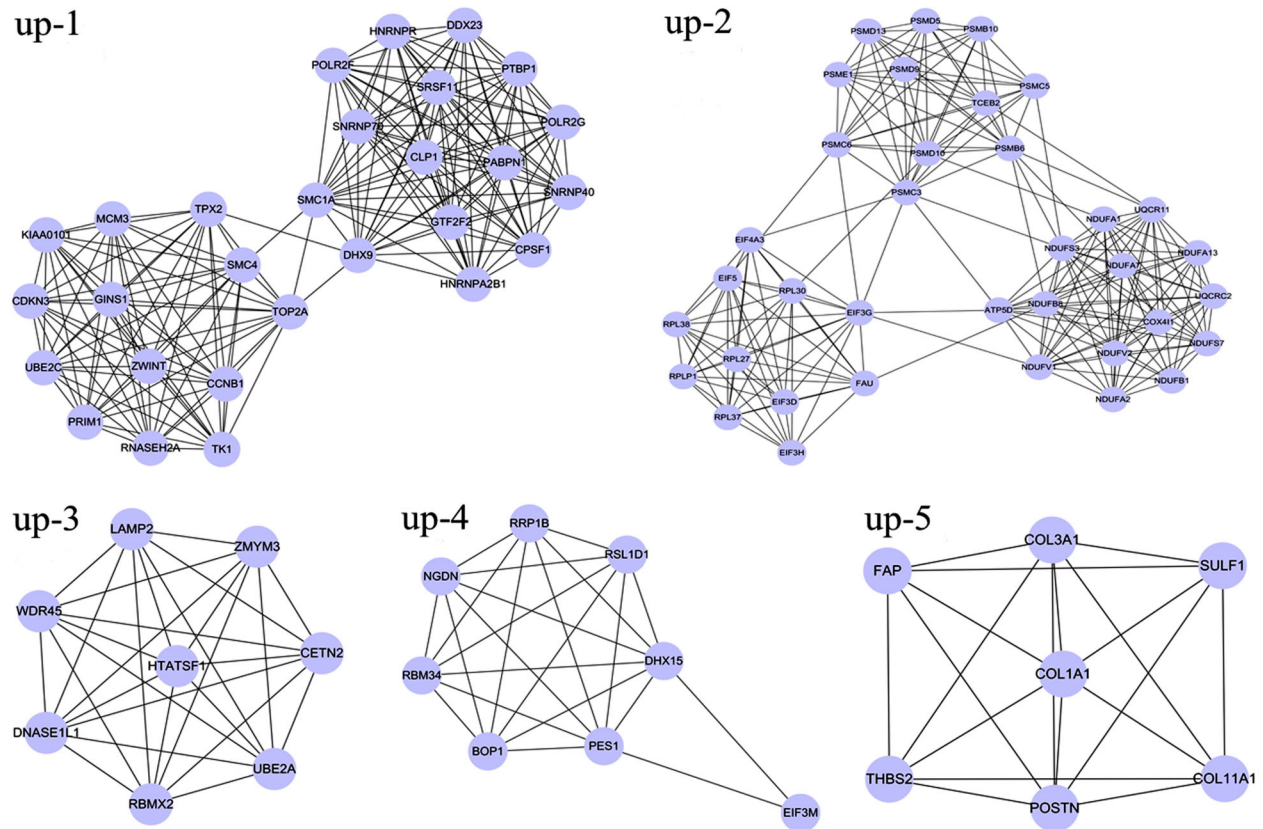


Figure 3. Modules of the protein-protein interaction network for upregulated differentially expressed genes.

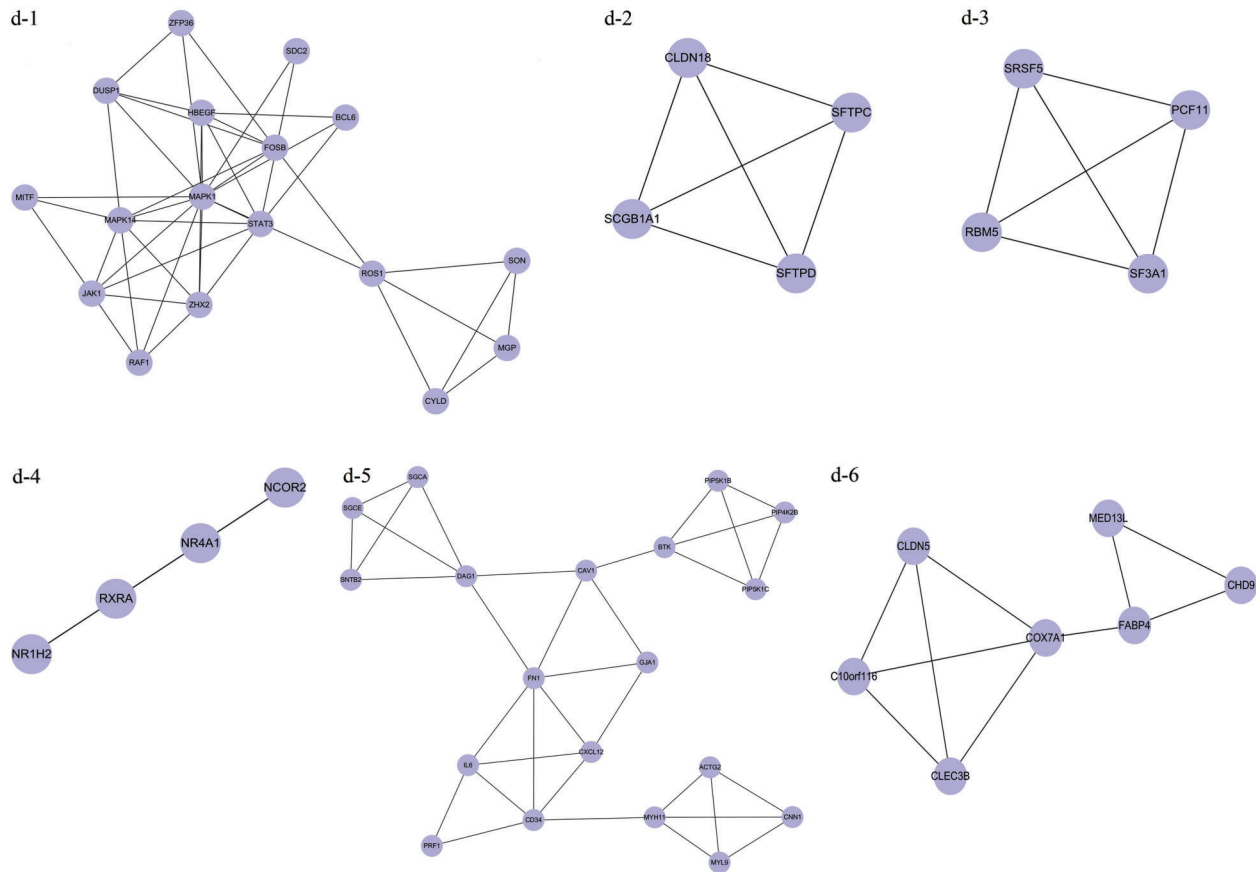


Figure 4. Modules of the protein-protein interaction network for downregulated differentially expressed genes.

were enriched for genes in the module d-1 (*MAPK1*, *MITF*, *RAF1*, *JAK1*, and *STAT3*): pancreatic cancer ($P=5.47E-04$), melanoma ($P=8.52E-03$), melanogenesis ($P=1.48E-02$), acute myeloid leukemia ($P=7.67E-03$), and cancer pathways ($P=3.69E-03$). Four pathways were enriched for genes in module d-5 (e.g., *PIP5K1B*, *PIP5K1C*, *FN1*, and *PIP4K2B*): regulation of the actin cytoskeleton ($P=4.61E-03$), inositol phosphate metabolism ($P=1.56E-02$), the phosphatidylinositol signaling system ($P=2.90E-02$), and Fc gamma R-mediated phagocytosis ($P=4.57E-02$; Table 5).

Discussion

In this study, 535 genes were identified as significantly upregulated and 465 as downregulated in lung adenocarcinoma samples compared with normal adjacent tissue samples. Based on functional and pathway enrichment analyses of two upregulated modules, the identified DEGs (*ATP5D*, *UQCRC2*, *NDUFA2*, *NDUFB8*, *NDUFA7*, *NDUFA1*, *NDUFB1*, *NDUFS7*, *UQCR11*, *NDUFV1*, *NDUFV2*, and *NDUFS3*) were mainly related to mitochondrial ATP synthesis coupled electron transport, the respiratory electron

transport chain, and mitochondrial electron transport. These genes were therefore enriched in the oxidative phosphorylation pathway.

DEGs such as *NDUFA2*, *NDUFB8*, *NDUFA7*, *NDUFA1*, *NDUFB1*, *NDUFS7*, *NDUFV1*, *NDUFV2*, and *NDUFS3* jointly encode subunits of nicotinamide adenine dinucleotide (NADH):ubiquinone oxidoreductase (complex I) (23). NADH is the entry enzyme of mitochondrial oxidative phosphorylation (24), which plays a key role in mitochondrial respiration. Mitochondrial respiration is thought to be vital to the bioenergetics of cancer cells, with breast, glioma, and cervical cancer cells shown to be highly reliant on mitochondrial respiration for ATP generation (25–27). It was also shown that mitochondrial respiration is substantially enhanced in NSCLC cells (28), while inhibition of mitochondrial electron transport prevents the growth of human lung cancer A549 cells (29). *NDUFS1* is already considered to be a prognostic marker for NSCLC (30), so we predict that the DEGs *NDUFA2*, *NDUFB8*, *NDUFA7*, *NDUFA1*, *NDUFB1*, *NDUFS7*, *NDUFV1*, *NDUFV2*, and *NDUFS3* play an important role in lung adenocarcinoma carcinogenesis, and may become diagnostic markers for lung cancer. However, this should be confirmed

Table 2. Enriched functions for genes in upregulated modules with a higher enrichment score.

Module/Term	Description	Count	P	DEGs
up-1				
GO:0000375	RNA splicing, via transesterification reactions	14	1.53E-17	<i>PABPN1, POLR2G, DHX9, POLR2F, HNRNPA2B1, PTBP1, HNRNPR, DDX23, CLP1, GTF2F2...</i>
GO:0000377	RNA splicing, via transesterification reactions with bulged adenosine as nucleophile	14	1.53E-17	<i>PABPN1, POLR2G, DHX9, POLR2F, HNRNPA2B1, PTBP1, HNRNPR, DDX23, CLP1, GTF2F2...</i>
GO:0000398	Nuclear mRNA splicing, via spliceosome	14	1.53E-17	<i>PABPN1, POLR2G, DHX9, POLR2F, HNRNPA2B1, PTBP1, HNRNPR, DDX23, CLP1, GTF2F2...</i>
GO:0008380	RNA splicing	14	1.03E-14	<i>PABPN1, POLR2G, DHX9, POLR2F, HNRNPA2B1, PTBP1, HNRNPR, DDX23, CLP1, GTF2F2...</i>
GO:0006397	mRNA processing	14	3.94E-14	<i>PABPN1, POLR2G, DHX9, POLR2F, HNRNPA2B1, PTBP1, HNRNPR, DDX23, CLP1, GTF2F2...</i>
GO:0016071	mRNA metabolic process	14	2.19E-13	<i>PABPN1, POLR2G, DHX9, POLR2F, HNRNPA2B1, PTBP1, HNRNPR, DDX23, CLP1, GTF2F2...</i>
GO:0006396	RNA processing	14	7.55E-12	<i>PABPN1, POLR2G, DHX9, POLR2F, HNRNPA2B1, PTBP1, HNRNPR, DDX23, CLP1, GTF2F2...</i>
up-2				
GO:0006119	Oxidative phosphorylation	12	3.69E-15	<i>UQCRC2, ATP5D, NDUFS7, NDUFA2, UQCR11, NDUFB8, NDUFV1, NDUFV2, NDUFA7, NDUFS3...</i>
GO:0042775	Mitochondrial ATP synthesis coupled electron transport	10	1.12E-14	<i>NDUFS7, NDUFA2, UQCR11, NDUFB8, NDUFV1, NDUFV2, NDUFA7, NDUFS3, NDUFA1, NDUFB1</i>
GO:0042773	ATP synthesis coupled electron transport	10	1.12E-14	<i>NDUFS7, NDUFA2, UQCR11, NDUFB8, NDUFV1, NDUFV2, NDUFA7, NDUFS3, NDUFA1, NDUFB1</i>
GO:0022904	Respiratory electron transport chain	10	7.35E-14	<i>NDUFS7, NDUFA2, UQCR11, NDUFB8, NDUFV1, NDUFV2, NDUFA7, NDUFS3, NDUFA1, NDUFB1</i>
GO:0006120	Mitochondrial electron transport, NADH to ubiquinone	9	9.94E-14	<i>NDUFS7, NDUFA2, NDUFB8, NDUFV1, NDUFV2, NDUFA7, NDUFS3, NDUFA1, NDUFB1</i>
GO:0045333	Cellular respiration	11	2.95E-13	<i>UQCRC2, NDUFS7, NDUFA2, UQCR11, NDUFB8, NDUFV1, NDUFV2, NDUFA7, NDUFS3, NDUFA1...</i>
GO:0022900	Electron transport chain	11	3.41E-13	<i>UQCRC2, NDUFS7, NDUFA2, UQCR11, NDUFB8, NDUFV1, NDUFV2, NDUFA7, NDUFS3, NDUFA1...</i>
GO:0015980	Energy derivation by oxidation of organic compounds	11	2.93E-11	<i>UQCRC2, NDUFS7, NDUFA2, UQCR11, NDUFB8, NDUFV1, NDUFV2, NDUFA7, NDUFS3, NDUFA1...</i>
GO:0006091	Generation of precursor metabolites and energy	13	1.87E-10	<i>ATP5D, UQCRC2, NDUFA2, NDUFB8, NDUFA7, COX4I1, NDUFA1, NDUFB1, NDUFS7, UQCR11...</i>
GO:0055114	Oxidation reduction	11	6.10E-06	<i>UQCRC2, NDUFS7, NDUFA2, UQCR11, NDUFB8, NDUFV1, NDUFV2, NDUFA7, NDUFS3, NDUFA1...</i>
GO:0016310	Phosphorylation	12	3.35E-05	<i>UQCRC2, ATP5D, NDUFS7, NDUFA2, UQCR11, NDUFB8, NDUFV1, NDUFV2, NDUFA7, NDUFS3...</i>
GO:0006793	Phosphorus metabolic process	12	1.78E-04	<i>UQCRC2, ATP5D, NDUFS7, NDUFA2, UQCR11, NDUFB8, NDUFV1, NDUFV2, NDUFA7, NDUFS3...</i>
GO:0006796	Phosphate metabolic process	12	1.78E-04	<i>UQCRC2, ATP5D, NDUFS7, NDUFA2, UQCR11, NDUFB8, NDUFV1, NDUFV2, NDUFA7, NDUFS3...</i>

GO: gene ontology; DEGs: differentially expressed genes.

in future in-depth studies. Similarly, *UQCRC2* and *UQCR11* may contribute to the occurrence of lung adenocarcinoma. They encode the ubiquinol-cytochrome c reductase complex, which is responsible for carrying electrons from ubiquinol to cytochrome c in the mitochondrial respiratory chain (31).

Moreover, *ATP5D*, which encodes a subunit of mitochondrial ATP synthase, is associated with mitochondrial ATP synthesis coupled electron transport in lung adenocarcinoma cells (32).

DEGs such as *PRIM1*, *MCM3*, and *RNASEH2A*, related to DNA replication, were also upregulated in lung

Table 3. Enriched KEGG pathways for genes in upregulated modules with a higher enrichment score.

Module/Term	Description	Count	P	DEGs
up-1				
hsa00240	Pyrimidine metabolism	4	1.15E-03	<i>PRIM1, POLR2G, POLR2F, TK1</i>
hsa03030	DNA replication	3	5.24E-03	<i>PRIM1, MCM3, RNASEH2A</i>
hsa03040	Spliceosome	3	4.41E-02	<i>DDX23, SNRNP40, SNRNP70</i>
up-2				
hsa00190	Oxidative phosphorylation	13	3.31E-13	<i>ATP5D, UQCRC2, NDUFA2, NDUFB8, NDUFA7, COX4I1, NDUFA1,</i>
hsa05012	Parkinson's disease	13	3.81E-13	<i>NDUFB1, NDUFS7, UQCR11, NDUFV1, NDUFV2, NDUFS3</i>
hsa05010	Alzheimer's disease	13	3.25E-11	
hsa05016	Huntington's disease	13	7.35E-11	
hsa03050	Proteasome	7	3.50E-07	<i>PSMB10, PSMC6, PSMD13, PSMB6, PSMC5, PSME1, PSMC3</i>
hsa03010	Ribosome	6	2.09E-04	<i>RPL30, RPLP1, RPL27, FAU, RPL37, RPL38</i>

KEGG: Kyoto Encyclopedia of Genes and Genomes; DEGs: differentially expressed genes.

Table 4. Enriched functions for genes in downregulated modules with a higher enrichment score.

Module/Term	Description	Count	P	DEGs
d-1 (Enrichment score = 2.57)				
GO:0007166	Cell surface receptor linked signal transduction	8	1.71E-03	<i>MAPK1, MAPK14, MITF, RAF1, JAK1, HBEGF, ROS1, STAT3</i>
GO:0007167	Enzyme linked receptor protein signaling pathway	5	2.02E-03	<i>RAF1, JAK1, HBEGF, ROS1, STAT3</i>
GO:0007169	Transmembrane receptor protein tyrosine kinase signaling pathway	4	5.64E-03	<i>RAF1, HBEGF, ROS1, STAT3</i>
d-1 (Enrichment score = 2.05)				
GO:0007166	Cell surface receptor linked signal transduction	8	1.71E-03	<i>MAPK1, MAPK14, MITF, RAF1, JAK1, HBEGF, ROS1, STAT3</i>
GO:0007242	Intracellular signaling cascade	7	4.96E-03	<i>ZFP36, MAPK1, DUSP1, MAPK14, RAF1, JAK1, STAT3</i>
GO:0006793	Phosphorus metabolic process	6	9.78E-03	<i>MAPK1, DUSP1, MAPK14, RAF1, JAK1, ROS1</i>
GO:0006796	Phosphate metabolic process	6	9.78E-03	<i>MAPK1, DUSP1, MAPK14, RAF1, JAK1, ROS1</i>
GO:0006468	Protein amino acid phosphorylation	5	1.42E-02	<i>MAPK1, MAPK14, RAF1, JAK1, ROS1</i>
GO:0007265	Ras protein signal transduction	3	1.44E-02	<i>MAPK1, MAPK14, RAF1</i>
GO:0016310	Phosphorylation	5	2.54E-02	<i>MAPK1, MAPK14, RAF1, JAK1, ROS1</i>
d-5 (Enrichment score = 2.22)				
GO:0046488	Phosphatidylinositol metabolic process	3	4.24E-04	<i>PIP5K1B, PIP5K1C, PIP4K2B</i>
GO:0046486	Glycerolipid metabolic process	4	1.88E-03	<i>CAV1, PIP5K1B, PIP5K1C, PIP4K2B</i>
GO:0030384	Phosphoinositide metabolic process	3	5.23E-03	<i>PIP5K1B, PIP5K1C, PIP4K2B</i>
GO:0006650	Glycerophospholipid metabolic process	3	1.38E-02	<i>PIP5K1B, PIP5K1C, PIP4K2B</i>
GO:0006644	Phospholipid metabolic process	3	2.76E-02	<i>PIP5K1B, PIP5K1C, PIP4K2B</i>
GO:0019637	Organophosphate metabolic process	3	3.12E-02	<i>PIP5K1B, PIP5K1C, PIP4K2B</i>
d-5 (Enrichment score = 1.83)				
GO:0032989	Cellular component morphogenesis	5	3.71E-03	<i>MYH11, GJA1, PIP5K1C, CXCL12, FN1</i>
GO:0031175	Neuron projection development	4	9.35E-03	<i>IL6, GJA1, PIP5K1C, CXCL12</i>
GO:0048666	Neuron development	4	1.90E-02	<i>IL6, GJA1, PIP5K1C, CXCL12</i>
GO:0000902	Cell morphogenesis	4	2.06E-02	<i>GJA1, PIP5K1C, CXCL12, FN1</i>
GO:0030030	Cell projection organization	4	2.16E-02	<i>IL6, GJA1, PIP5K1C, CXCL12</i>
GO:0030182	Neuron differentiation	4	3.39E-02	<i>IL6, GJA1, PIP5K1C, CXCL12</i>

GO: gene ontology; DEGs: differentially expressed genes.

Table 5. Enriched KEGG pathways for genes in downregulated modules with a higher enrichment score.

Module/Term	Description	Count	P	DEGs
d-1 (Enrichment score = 2.60)				
hsa05212	Pancreatic cancer	4	5.47E-04	<i>MAPK1, RAF1, JAK1, STAT3</i>
hsa05200	Pathways in cancer	5	3.69E-03	<i>MAPK1, MITF, RAF1, JAK1, STAT3</i>
hsa05221	Acute myeloid leukemia	3	7.67E-03	<i>MAPK1, RAF1, STAT3</i>
d-1 (Enrichment score = 2.11)				
hsa05200	Pathways in cancer	5	3.69E-03	<i>MAPK1, MITF, RAF1, JAK1, STAT3</i>
hsa05218	Melanoma	3	8.52E-03	<i>MAPK1, MITF, RAF1</i>
hsa04916	Melanogenesis	3	1.48E-02	<i>MAPK1, MITF, RAF1</i>
d-5 (Enrichment score = 1.76)				
hsa04810	Regulation of actin cytoskeleton	5	4.61E-03	<i>PIP5K1B, PIP5K1C, FN1, PIP4K2B, MYL9</i>
hsa00562	Inositol phosphate metabolism	3	1.56E-02	<i>PIP5K1B, PIP5K1C, PIP4K2B</i>
hsa04070	Phosphatidylinositol signaling system	3	2.90E-02	<i>PIP5K1B, PIP5K1C, PIP4K2B</i>
hsa04666	Fc gamma R-mediated phagocytosis	3	4.57E-02	<i>PIP5K1B, PIP5K1C, PIP4K2B</i>

KEGG: Kyoto Encyclopedia of Genes and Genomes; DEGs: differentially expressed genes.

adenocarcinoma cells in the present study. Lung adenocarcinoma is a form of solid tumor, and its biological behavior including formation, development, and attack is closely related to abnormal cell proliferation, which includes DNA replication. *PRIM1* encodes one of the subunits (p49) of the eukaryotic primase, which is a heterodimer consisting of a small and a large subunit that synthesizes RNA primers for the Okazaki fragments during discontinuous DNA replication (33). *MCM3* encodes a major control factor in eukaryotic DNA replication initiation and extension (34,35), while *RNASEH2A* codes for a subunit of the ribonuclease H2 complex which helps break down RNA from RNA-DNA hybrids formed during DNA replication (36). Therefore, these identified DEGs are thought to play important roles in lung adenocarcinoma.

Some DEGs in downregulated modules, such as *MAPK1*, *STAT3*, *RAF1*, and *JAK1*, are enriched in cell surface receptor linked signal transduction and the enzyme linked receptor protein signaling pathway. *MAPK1* in the MAPK family is also known as extracellular signal-regulated kinase2 (ERK2), and is involved in cell proliferation. Moreover, the ERK pathway is known to be activated during the early stages of lung adenocarcinoma (37,38). *RAF* is a proto-oncogene, encoding a serine/threonine protein kinase that functions in the highly conserved Ras-Raf-MEK-ERK signal transduction pathway, and provides an important link between Ras and ERK signaling activation. *RAF1* in the *RAF* family encodes *Raf1* kinase, which is reported to be expressed abnormally in

human lung adenocarcinomas (39). Finally, the JAK/STAT3 signaling pathway plays an essential part in the formation of NSCLC (40). Hence, it appears that these genes might be involved in the formation and development of lung adenocarcinoma.

In conclusion, we have identified DEGs that might be involved in the pathogenesis of lung adenocarcinoma. In particular, the upregulated DEGs (e.g., *PRIM1*, *MCM3*, *RNASEH2A*, *UQCRC2*, *UQCR11*, *ATP5D*, *PRIM1*, *MCM3*, *RNASEH2A*, and DEGs encoding subunits of NADH) and downregulated DEGs (e.g., *MAPK1*, *STAT3*, *RAF1*, and *JAK1*) in network modules related to important functions and pathways might provide novel insights into the molecular mechanisms underlying lung adenocarcinoma and serve as therapeutic targets. However, our findings should be confirmed by further experiments, and lung adenocarcinoma at different stages should be investigated.

Supplementary Material

[Click here to view \[pdf\]](#)

Acknowledgements

We thank Harbin Medical University College of Bioinformatics Science and Technology for help with the analysis of biological information data. This study was funded by the Health and Family Planning Commission of Heilongjiang Province (Grant #2014-359).

References

- Chen WQ, Zhang SW, Zou XN. Estimation and projection of lung cancer incidence and mortality in China. *Chin J Lung Cancer* 2010; 13: 488–493.
- Parkin DM, Bray F, Ferlay J, Pisani P. Global cancer statistics, 2002. *CA Cancer J Clin* 2005; 55: 74–108, doi: 10.3322/canjclin.55.2.74.
- Kris M, Johnson B, Kwiatkowski D, Iafrate A, Wistuba I, Aronson S, et al. Identification of driver mutations in tumor specimens from 1,000 patients with lung adenocarcinoma: The NCI's Lung Cancer Mutation Consortium (LCMC). *J Clin Oncol* 2011; 29 (15 Suppl).
- Mollberg N, Surati M, Demchuk C, Fathi R, Salama AK, Husain AN, et al. Mind-mapping for lung cancer: towards a personalized therapeutics approach. *Adv Ther* 2011; 28: 173–194, doi: 10.1007/s12325-010-0103-9.
- Van Damme N, Deron P, Van Roy N, Demetter P, Bols A, Van Dorpe J, et al. Epidermal growth factor receptor and K-RAS status in two cohorts of squamous cell carcinomas. *BMC Cancer* 2010; 10: 189, doi: 10.1186/1471-2407-10-189.
- Forbes S, Clements J, Dawson E, Bamford S, Webb T, Dogan A, et al. COSMIC 2005. *Br J Cancer* 2006; 94: 318–322, doi: 10.1038/sj.bjc.6602928.
- Mills NE, Fishman CL, Scholes J, Anderson SE, Rom WN, Jacobson DR. Detection of K-ras oncogene mutations in bronchoalveolar lavage fluid for lung cancer diagnosis. *J Natl Cancer Inst* 1995; 87: 1056–1060, doi: 10.1093/jnci/87.14.1056.
- Zhang X, Zhang S, Yang X, Yang J, Zhou Q, Yin L, et al. Fusion of EML4 and ALK is associated with development of lung adenocarcinomas lacking EGFR and KRAS mutations and is correlated with ALK expression. *Mol Cancer* 2010; 9: 188, doi: 10.1186/1476-4598-9-188.
- Chapman PB, Hauschild A, Robert C, Haanen JB, Ascierto P, Larkin J, et al. Improved survival with vemurafenib in melanoma with BRAF V600E mutation. *N Engl J Med* 2011; 364: 2507–2516, doi: 10.1056/NEJMoa1103782.
- Takeuchi K, Soda M, Togashi Y, Suzuki R, Sakata S, Hatano S, et al. RET, ROS1 and ALK fusions in lung cancer. *Nat Med* 2012; 18: 378–381, doi: 10.1038/nm.2658.
- Jun HJ, Johnson H, Bronson RT, de Feraudy S, White F, Charest A. The oncogenic lung cancer fusion kinase CD74-ROS activates a novel invasiveness pathway through E-Syt1 phosphorylation. *Cancer Res* 2012; 72: 3764–3774, doi: 10.1158/0008-5472.CAN-11-3990.
- Friboulet L, Olaussen KA, Pignon JP, Shepherd FA, Tsao MS, Graziano S, et al. ERCC1 isoform expression and DNA repair in non-small-cell lung cancer. *N Engl J Med* 2013; 368: 1101–1110, doi: 10.1056/NEJMoa1214271.
- Kohno S, Kitajima S, Sasaki N, Muranaka H, Takahashi C. Abstract LB-130: The metabolic function of RB tumor suppressor gene. *Cancer Research* 2013; 73 (8 Supplement): LB-130, doi: 10.1158/1538-7445.AM2013-LB-130.
- Heavey S, O'Byrne KJ, Gately K. Strategies for co-targeting the PI3K/AKT/mTOR pathway in NSCLC. *Cancer Treat Rev* 2014; 40: 445–456, doi: 10.1016/j.ctrv.2013.08.006.
- Minami D, Takigawa N, Takeda H, Takata M, Ochi N, Ichihara E, et al. PTEN deficient lung cancer cells are sensitive to the combination of olaparib with cisplatin through suppressing DNA damage signaling. *Cancer Research* 2013; 73 (8 Supplement): 2048, doi: 10.1158/1538-7445.AM2013-2048.
- Marks JL, Gong Y, Chitale D, Golas B, McLellan MD, Kasai Y, et al. Novel MEK1 mutation identified by mutational analysis of epidermal growth factor receptor signaling pathway genes in lung adenocarcinoma. *Cancer Res* 2008; 68: 5524–5528, doi: 10.1158/0008-5472.CAN-08-0099.
- Stearman RS, Dwyer-Nield L, Zerbe L, Blaine SA, Chan Z, Bunn PA Jr, et al. Analysis of orthologous gene expression between human pulmonary adenocarcinoma and a carcinogen-induced murine model. *Am J Pathol* 2005; 167: 1763–1775, doi: 10.1016/S0002-9440(10)61257-6.
- Wu Z, Irizarry R A, Gentleman R, Martinez-Murillo F, Spencer F. A model-based background adjustment for oligonucleotide expression arrays. *J Amer Statist Assoc* 2004; 99: 909–917, doi: 10.1198/01621450400000683.
- Benjamini Y, Hochberg Y. Controlling the false discovery rate: a practical and powerful approach to multiple testing. *J R Stat Soc Ser B Stat Methodol* 1995; 289–300.
- Kanehisa M, Goto S. KEGG: kyoto encyclopedia of genes and genomes. *Nucleic Acids Res* 2000; 28: 27–30, doi: 10.1093/nar/28.1.27.
- Lamb J, Crawford ED, Peck D, Modell JW, Blat IC, Wrobel MJ, et al. The Connectivity Map: using gene-expression signatures to connect small molecules, genes, and disease. *Science* 2006; 313: 1929–1935, doi: 10.1126/science.1132939.
- He X, Zhang J. Why do hubs tend to be essential in protein networks? *PLoS Genet* 2006; 2: e88, doi: 10.1371/journal.pgen.0020088.
- Emahazion T, Brookes AJ. Mapping of the NDUFA2, NDUFA6, NDUFA7, NDUFB8, and NDUFS8 electron transport chain genes by intron based radiation hybrid mapping. *Cytogenet Cell Genet* 1998; 82: 114, doi: 10.1159/000015081.
- Nakamaru-Ogiso E, Han H, Matsuno-Yagi A, Keinan E, Sinha SC, Yagi T, et al. The ND2 subunit is labeled by a photo-affinity analogue of asimicin, a potent complex I inhibitor. *FEBS Lett* 2010; 584: 883–888, doi: 10.1016/j.febslet.2010.01.004.
- Guppy M, Leedman P, Zu X, Russell V. Contribution by different fuels and metabolic pathways to the total ATP turnover of proliferating MCF-7 breast cancer cells. *Biochem J* 2002; 364: 309–315, doi: 10.1042/bj3640309.
- Griguer CE, Oliva CR, Gillespie GY. Glucose metabolism heterogeneity in human and mouse malignant glioma cell lines. *J Neurooncol* 2005; 74: 123–133, doi: 10.1007/s11060-004-6404-6.
- Herst PM, Berridge MV. Cell surface oxygen consumption: a major contributor to cellular oxygen consumption in glycolytic cancer cell lines. *Biochim Biophys Acta* 2007; 1767: 170–177, doi: 10.1016/j.bbabi.2006.11.018.
- Hooda J, Cadinu D, Alam MM, Shah A, Cao TM, Sullivan LA, et al. Enhanced heme function and mitochondrial respiration promote the progression of lung cancer cells. *PLoS One* 2013; 8: e63402, doi: 10.1371/journal.pone.0063402.
- Han YH, Kim SH, Kim SZ, Park WH. Antimycin A as a mitochondrial electron transport inhibitor prevents the growth of human lung cancer A549 cells. *Oncol Rep* 2008; 20: 689–693.
- Su CY, Hsiao M. NDUFS1 as a prognostic marker in lung cancer: a clinicopathological analysis of 106 cases of non-small cell lung cancer. *FASEB J* 2013; 27: 58.57.

31. Miyake N, Yano S, Sakai C, Hatakeyama H, Matsushima Y, Shiina M, et al. Mitochondrial complex III deficiency caused by a homozygous UQCRC2 mutation presenting with neonatal-onset recurrent metabolic decompensation. *Hum Mutat* 2013; 34: 446–452, doi: 10.1002/humu.22257.
32. Chen G, Gharib TG, Huang CC, Thomas DG, Shedden KA, Taylor JM, et al. Proteomic analysis of lung adenocarcinoma: identification of a highly expressed set of proteins in tumors. *Clin Cancer Res* 2002; 8: 2298–2305.
33. Copeland WC, Tan X. Active site mapping of the catalytic mouse primase subunit by alanine scanning mutagenesis. *J Biol Chem* 1995; 270: 3905–3913, doi: 10.1074/jbc.270.8.3905.
34. Bell SP, Dutta A. DNA replication in eukaryotic cells. *Annu Rev Biochem* 2002; 71: 333–374, doi: 10.1146/annurev.biochem.71.110601.135425.
35. Schwacha A, Bell SP. Interactions between two catalytically distinct MCM subgroups are essential for coordinated ATP hydrolysis and DNA replication. *Mol Cell* 2001; 8: 1093–1104, doi: 10.1016/S1097-2765(01)00389-6.
36. Crow YJ, Leitch A, Hayward BE, Garner A, Parmar R, Griffith E, et al. Mutations in genes encoding ribonuclease H2 subunits cause Aicardi-Goutieres syndrome and mimic congenital viral brain infection. *Nat Genet* 2006; 38: 910–916, doi: 10.1038/ng1842.
37. Voisin L, Saba-Ei-Leil MK, Julien C, Fremin C, Meloche S. Genetic demonstration of a redundant role of extracellular signal-regulated kinase 1 (ERK1) and ERK2 mitogen-activated protein kinases in promoting fibroblast proliferation. *Mol Cell Biol* 2010; 30: 2918–2932, doi: 10.1128/MCB.00131-10.
38. Lopez-Malpartida AV, Ludena MD, Varela G, Garcia PJ. Differential ErbB receptor expression and intracellular signaling activity in lung adenocarcinomas and squamous cell carcinomas. *Lung Cancer* 2009; 65: 25–33, doi: 10.1016/j.lungcan.2008.10.009.
39. Powell CA, Spira A, Derti A, DeLisi C, Liu G, Borczuk A, et al. Gene expression in lung adenocarcinomas of smokers and nonsmokers. *Am J Respir Cell Mol Biol* 2003; 29:157–162, doi: 10.1165/rcmb.2002-0183RC.
40. Song L, Rawal B, Nemeth JA, Haura EB. JAK1 activates STAT3 activity in non-small-cell lung cancer cells and IL-6 neutralizing antibodies can suppress JAK1-STAT3 signaling. *Mol Cancer Ther* 2011; 10: 481–494, doi: 10.1158/1535-7163.MCT-10-0502.